Received July 20, 2017, accepted August 14, 2017, date of publication August 29, 2017, date of current version September 19, 2017.

Digital Object Identifier 10.1109/ACCESS.2017.2745416

Exploiting Polarization for System Capacity Maximization in Ultra-Dense Small Cell Networks

SHUO CHEN[1], (Student Member, IEEE), ZHIMIN ZENG[1,2], AND CAILI GUO[1,2], (Senior Member, IEEE)

[1]Beijing Key Laboratory of Network System Architecture and Convergence, School of Information and Communication Engineering, Beijing University of Posts and Telecommunications, Beijing 100876, China

[2]Beijing Laboratory of Advanced Information Networks, Beijing 100876, China

Corresponding author: Caili Guo (guocaili@bupt.edu.cn)

This work was supported in part by the National Natural Science Foundation of China under Grant 61571062 and Grant 61271177, in part by the Fundamental Research Funds for the Central Universities under Grant 2014ZD03-01, and in part by the Postgraduate Innovation Fund of the School of Information and Communication Engineering, Beijing University of Posts and Telecommunications, 2015.

ABSTRACT Ultra-dense deployment of small cell networks is widely regarded as a key role to meet the increasing demand for huge capacity of wireless communication systems. Meanwhile, network densification will result in severe inter-cell interference and thus impair system performance. Traditional radio resource management schemes pay attention to interference mitigation through resource allocation in time, frequency, space, and power domains, or a mix of them. In this paper, polarization, an important and underutilized property of electromagnetic waves, is exploited as a novel means to enhance system capacity. We propose a multicell joint polarization, power and subcarrier allocation (MC-JPPSA) scheme to maximize system capacity through joint optimization of transmitting polarization states, power, and subcarriers with an iterative approach. Though the iterative solution is suboptimal, simulation results demonstrate that MC-JPPSA scheme can strike a balance between performance and complexity compared with the optimal exhaustive search. Furthermore, the proposed scheme outperforms traditional joint power and subcarrier allocation schemes by means of exploiting polarization in ultra-dense small cell networks.

INDEX TERMS Ultra-dense small cell networks, system capacity, radio resource management, polarization.

I. INTRODUCTION

The proliferation of smart devices and rapid development of wireless services have led to exponential growth of mobile traffic volume and triggered an explosively increasing demand for high-date-rate services in mobile communication networks. According to the prediction of Cisco, global mobile data traffic will increase 8-fold for the period 2015-2020 [1]. Due to limited spectrum resources, traditional cell division techniques are no longer applicable facing the ever-growing traffic demand [2]. In order to boost system capacity and ensure user experience, the ultra-dense deployment of small cells is regarded as a key role in future fifth generation (5G) networks. Benefited from the close transmitter-receiver proximity, small cells can enhance spatial reuse, achieve high signal-to-interference-plus-noise ratio (SINR) and improve spectral efficiency with low transmitting power [3].

Although such ultra-dense deployment of small cells holds great potential for high spectral efficiency, challenges coming with spatial and frequency reuse result in severe interference problem. With orthogonal frequency-division multiple access (OFDMA) technology, the intra-cell interference is eliminated among user equipments (UEs) in the same cell since a subcarrier is assigned to at most one UE at a time [4]. However, small cells are deployed based on a user-deploying fashion, that is, users rather than service providers install small cells by themselves without network planning. The coverage of a small cell may be overlapped by that of neighboring cells, which gives rise to severe inter-cell interference among small cells and significant performance degradation.

A. RELATED LITERATURE

Interference mitigation is essential for system performance enhancement in dense small cell networks by radio resource management (RRM). Traditional RRM schemes in dense small cell networks pay attention to resource allocation in time, frequency, space and power domains, or a mix of them.

In time domain, dynamic almost blank sub-frame (ABS) technologies are utilized to mitigate interference by allocating ABS, protected sub-frame, or non-protected sub-frame to each small cell base station (SBS) dynamically [5]. RRM in time domain faces the challenge that the number of ABS assignments increases and available resources of each SBS decrease in dense deployment scenario. The RRM in frequency domain exploits the assignment of orthogonal frequency channels among small cells to avoid inter-cell interference. When small cells become denser, recent studies pay attention to the balance between orthogonal assignment and frequency reuse to strive for high spectral efficiency [6] at the price of increased interference. In space domain, RRM is done by taking advantage of MIMO and massive MIMO systems [7] in dense small cell networks and limited by high hardware requirement and algorithm complexity. Power control is a substantially studied method to enhance system performance by allocating transmitting power of small cells characterized by low-power consumption [8]; however, challenges come with limited power resource under stringent transmit-power constraint in dense deployment scenario.

Polarization, an inherent property of electromagnetic waves defined as the orientation of electric field vector, is an under-utilized resource in wireless communication. Over the past few decades, polarization has been intensively researched in optical fiber, radar and satellite communications [9]. In wireless communication systems, orthogonally dual-polarized antennas (ODPAs) have been widely employed owning to the great benefit of cost and space effectiveness [10], which promotes the development of polarization research in wireless communication. By leveraging polarization, additional degrees of freedom (DoFs) can be exploited as promising means to further enhance system capacity along with traditional time, frequency, space and power resources.

To date, motivated by the potential of polarization information processing, a series of polarization-based solutions to address interference problem have been put forward. The authors in [11]–[13] utilize additional DoFs introduced by polarization, and investigate polarization-based spectrum sharing to maximize link capacity and avoid harmful interference between two communication links in cognitive radio networks. The property of polarization orthogonality is utilized in [14] and [15] to enable orthogonal transmission of two networks and suppress interference between them. Cao *et al.* pay attention to polarization-based overlay spectrum sharing based on interference suppression via polarization zero-forcing and polarization filtering [16]–[18]. Although interference suppression technologies in polarization domain are suitable for multi-interference circumstance, they have strict requirements on the number of receiving antennas and thus fail to work in downlink communication scenario with severe interference.

In [19], we propose a polarization-based underlay spectrum sharing scheme in cognitive heterogeneous cellular network, which realizes the coexistence between small cell and macrocell by optimizing polarization states of small cell. Through exploiting spectrum opportunities in polarization and power domains simultaneously, the work of [19] is extended in [20] by jointly optimizing polarization states and transmitting power of small cell. Our studies in [19] and [20] reveal the benefit of exploiting polarization to avoid cross-tier interference and improve capacity in heterogeneous cellular networks.

However, in ultra-dense small cell networks with severe co-tier interference, the utilization of polarization resource has not been addressed in the existing literature. Jointly exploiting polarization and other resource domains is a promising research direction with high potential to mitigate co-tier multi-interference and further enhance system capacity.

B. PURPOSE OF THIS PAPER

In this work, we leverage polarization for ultra-dense small cell networks, and propose a multicell joint polarization, power and subcarrier allocation (MC-JPPSA) scheme to realize the coexistence among small cells. MC-JPPSA scheme jointly optimizes transmitting polarization state, power and subcarrier allocation with a centralized approach, which exploits spectrum opportunities in polarization domain for system capacity maximization. Since the resource allocation problem is a mixed integer non-convex problem with high computational complexity, we employ a three-step iterative method to derive the sub-optimal yet efficient solutions. Firstly, transmitting polarization states of SBSs are derived and generated via virtual polarization adaptation (VPA) method when power and subcarrier allocation is fixed. Secondly, given fixed polarization state and subcarrier allocation, the polarization-based power allocation is proposed to avoid the influence of polarization mismatch which degrades the performance of traditional iterative water filling solutions. Thirdly, to combat polarization mode dispersion (PMD) effect in wideband environments, subcarrier assignment is introduced so that polarization state and power is allocated for every subcarrier. Discussions of the proposed scheme are presented including computational complexity study, implementation issue and convergence analysis. Simulation results demonstrate the performance advantage of MC-JPPSA scheme in comparison with traditional joint power and subcarrier allocation scheme as well as existing joint polarization and power allocation scheme, which verifies the great potential of leveraging polarization in ultra-dense small cell networks to enhance system capacity.

C. PAPER ORGANIZATION AND NOTATIONS

The rest of this paper is organized as follows. Section II provides the system model of ultra-dense small cell networks, and the formulation of system capacity maximization problem. Section III presents the proposed MC-JPPSA scheme including transmit optimization and theoretical discussions. In Section IV, simulation results are provided and analyzed. Finally, this paper is concluded in Section V.

Notations: $(\cdot)'$ denotes complex conjugation. $(\cdot)^T$ and $(\cdot)^H$ represent transpose and conjugate transpose, respectively. $|x|$ is the absolute value of x. $[x]^+ =$ denotes x if $x > 0$ or 0 otherwise. $\|\cdot\|$ represents the Euclidean norm. $v_{\min}(\boldsymbol{X})$ denotes the eigenvector corresponding to the minimum eigenvalue of matrix $\boldsymbol{X}$.

II. SYSTEM MODEL AND PROBLEM FORMULATION

A. SYSTEM MODEL

In this paper, we consider a downlink ultra-dense small cell scenario where a number of small cells are densely deployed in small ranges with universal frequency reuse. OFDMA is adopted in each small cell to avoid intra-cell interference.

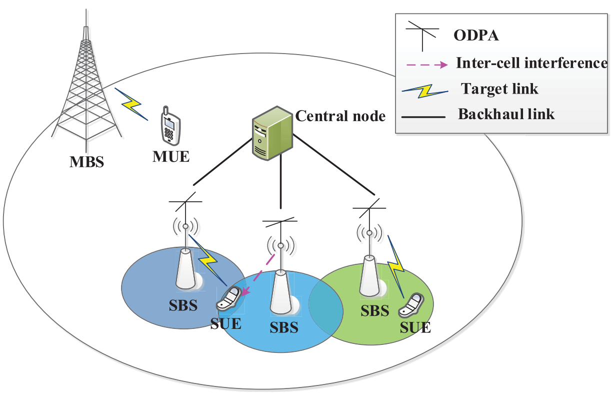

FIGURE 1. Coexistence scenario of ultra-dense small cell networks.

Fig. 1 illustrates the dense deployment scenario considered in this paper. The cross-tier interference from the downlink communication between macro base station (MBS) and macro user equipments (MUEs) is regarded as additive white Gaussian noise (AWGN) for simplicity to focus on co-tier interference mitigation. A set $\mathcal{L} = \{1, 2, \ldots, L\}$ of small cells is densely deployed and connected via backhaul to a central node which is responsible for information exchange with SBSs and making decisions of resource allocation. The density of SBSs is comparable to that of small cell user equipments (SUEs). The lth SBS employs equal-spaced subcarriers set $\mathcal{N} = \{1, 2, \ldots, N\}$ and serves M_l SUEs. The antennas equipped on SBSs are ODPAs, and those of SUEs are unspecified, that is, either uni-polarized antennas or ODPAs are feasible. The lth SBS conducts downlink communication at subcarrier n with transmitting polarization state $\boldsymbol{P}_{l,n,T}$ and power $G_{l,n}$ under transmit-power constraint. $\boldsymbol{P}_{l,n,T}$ is generated based on VPA method [21], and the receiving polarization state $\boldsymbol{P}_{l,n,R}$ is determined by antenna configurations of receiving antennas. The downlink communication in the lth small cell suffers inter-cell interference from other small cells sharing the same spectrum.

The transmitting polarization state $\boldsymbol{P}_{l,n,T}$ characterizes the orientation of the transmitted signal in the form of radiated electromagnetic wave. It contains polarization information and can be completely described by Jones vector as follows

$$\boldsymbol{P}_{l,n,T} = \begin{pmatrix} \cos\gamma_{l,n,T} \\ \sin\gamma_{l,n,T} e^{j\phi_{l,n,T}} \end{pmatrix} \tag{1}$$

where $\gamma_{l,n,T} \in [0, \pi/2]$ and $\phi_{l,n,T} \in [0, 2\pi]$ are amplitude ratio and relative phase descriptors, respectively. $(\gamma_{l,n,T}, \phi_{l,n,T})$, namely amplitude-phase descriptor, describes the amplitude ratio and phase difference between horizontally and vertically polarized electric-field components of the transmitted signal. Except for Jones vector, polarization information can also be represented by normalized instantaneous Stokes sub-vector defined as

$$\boldsymbol{S}_{l,n,T} = \begin{pmatrix} g_{1,l,n,T} \\ g_{2,l,n,T} \\ g_{3,l,n,T} \end{pmatrix} = \begin{pmatrix} \cos 2\gamma_{l,n,T} \\ \sin 2\gamma_{l,n,T}\cos\phi_{l,n,T} \\ \sin 2\gamma_{l,n,T}\sin\phi_{l,n,T} \end{pmatrix} \tag{2}$$

$\boldsymbol{P}_{l,n,T}$ is deflected during transmission due to depolarization effect of fading channels. In this paper, the channels are modeled as 2×2 dual-polarized frequency-selective fading channels incorporating depolarization effect according to the method in [22]. Channel matrix $\boldsymbol{H}_{m_l,l,n}$ represents the downlink channel from the lth SBS to the m_lth SUE at subcarrier n, and is denoted as

$$\boldsymbol{H}_{m_l,l,n} = \begin{pmatrix} \sum_{s=1}^{S} h^{HH}_{s,m_l,l,n} e^{j2\pi f_n \tau^H_{s,m_l,l,n}} & \sum_{q=1}^{Q} h^{VH}_{q,m_l,l,n} e^{j2\pi f_n \tau^V_{q,m_l,l,n}} \\ \sum_{s=1}^{S} h^{HV}_{s,m_l,l,n} e^{j2\pi f_n \tau^V_{s,m_l,l,n}} & \sum_{q=1}^{Q} h^{VV}_{q,m_l,l,n} e^{j2\pi f_n \tau^V_{q,m_l,l,n}} \end{pmatrix} \tag{3}$$

where f_n is the frequency of subcarrier n, S and Q are the numbers of multipaths associated with the H-polarized and V-polarized signal components, respectively. $h^{xy}_{i,m_l,l,n}$ denotes the complex channel gain between the x-polarized component of transmitted signal and y-polarized output signal component after transmission at the ith propagation path. $\tau^z_{i,m_l,l,n}$ represents the propagation delay for the z-polarized signal component for the ith propagation path.

The polarization state of output signal after transmission can be represented as

$$\boldsymbol{P}_{l,n,O} = \boldsymbol{H}_{m_l,l,n}\boldsymbol{P}_{l,n,T} \tag{4}$$

In (4), the output polarization state is a function of subcarrier frequency, and can be plotted on the Poincare sphere as shown in Fig. 2. Assuming that $\boldsymbol{P}_{l,n,T} = \boldsymbol{P}_t$, $\forall n \in \mathcal{N}$, transmitting polarization state $\boldsymbol{P}_t$ is represented as the green point on the Poincare sphere. After transmission, the output polarization state varies with subcarrier frequency, whose dispersion is presented as a spiral pattern. The dispersion of polarization state as a function of subcarrier frequency is referred to as polarization mode dispersion (PMD).

In view of the frequency-dependent characteristics of polarization, subcarrier-based polarization state optimization along with power and subcarrier allocation is preferable in this paper compared with band-based fashion in [19] and [20].

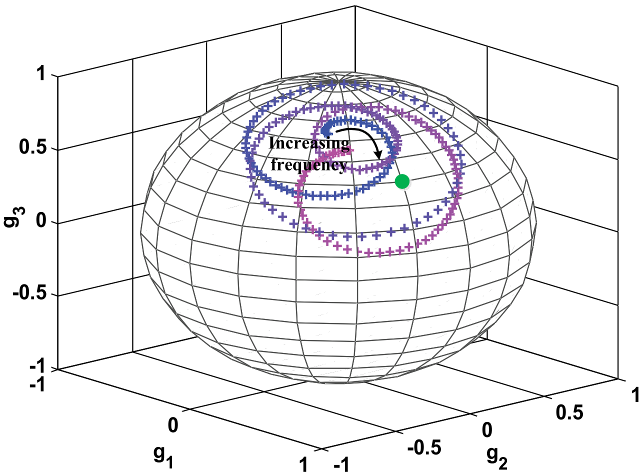

FIGURE 2. Output polarization states on the poincare sphere.

Time overhead and complexity can be easily reduced based on clustering at the cost of performance, which is beyond the scope of this paper.

B. PROBLEM FORMULATION

Assuming that SUE m_l is served by SBS l, its received signal at subcarrier n can be written as

$$r_{m_l,n} = \underbrace{\left(\boldsymbol{P}_{l,n,R}\right)^H \boldsymbol{H}_{m_l,l,n}\boldsymbol{P}_{l,n,T}s_{l,n}}_{\text{target signal}} + \underbrace{\sum_{i\neq l}^{L}\left(\boldsymbol{P}_{l,n,R}\right)^H \boldsymbol{H}_{m_l,i,n}\boldsymbol{P}_{i,n,T}s_{i,n}}_{\text{inter-cell interference}} + \underbrace{n_{m_l,n}}_{\text{noise}} \tag{5}$$

where $\boldsymbol{H}_{m_l,l,n}$ and $\boldsymbol{H}_{m_l,i,n}$ are assumed to be independent, flat at each subcarrier, and static during the resource allocation process. $s_{l,n}$ is the transmitted signal from SBS l at subcarrier n with transmitting power $G_{l,n}$. $G_{l,n}$ is assumed to satisfy $\sum_{n=1}^{N} G_{l,n} \leq G_{l,max}, \forall l \in \mathcal{L}$ where $G_{l,max}$ is the transmit-power constraint. $n_{m_l,n}$ denotes AWGN of SUE m_l at n with power ${\sigma_{m_l,n}}^2$.

The downlink capacity of SUE m_l at n is calculated mathematically by the Shannon's formula

$$C_{m_l,n} = \log_2\left(1+\frac{G_{l,n}\left|\left(\boldsymbol{P}_{l,n,R}\right)^H \boldsymbol{H}_{m_l,l,n}\boldsymbol{P}_{l,n,T}\right|^2}{\sigma^2_{m_l,n}+\sum_{i\neq l}^{L} G_{i,n}\left|\left(\boldsymbol{P}_{l,n,R}\right)^H \boldsymbol{H}_{m_l,i,n}\boldsymbol{P}_{i,n,T}\right|^2}\right) \tag{6}$$

This paper aims to devise an optimal joint polarization, power and subcarrier allocation scheme, which maximize the system capacity of ultra-dense small cell networks. Let binary variable $a_{m_l,n}$ denote the subcarrier allocation, where $a_{m_l,n} = 1$ indicates that subcarrier n is allocated to SUE m_l and $a_{m_l,n} = 0$ otherwise. We define $\boldsymbol{P}_T = \left(\boldsymbol{P}_{1,T}, \boldsymbol{P}_{2,T}, \cdots, \boldsymbol{P}_{L,T}\right)$ as the vector indicating the transmitting polarization states where $\boldsymbol{P}_{l,T} = (\boldsymbol{P}_{l,1,T}, \boldsymbol{P}_{l,2,T}, \cdots, \boldsymbol{P}_{l,N,T})^T$. We also use $\boldsymbol{G} = (\boldsymbol{G}_1, \boldsymbol{G}_2, \cdots, \boldsymbol{G}_L)$ where $\boldsymbol{G}_l = \left(G_{l,1}, G_{l,2}, \cdots, G_{l,N}\right)^T$, and $\boldsymbol{a} = (\boldsymbol{a}_{m_1}, \boldsymbol{a}_{m_2}, \cdots, \boldsymbol{a}_{m_L})$ where $\boldsymbol{a}_{m_l} = \left(a_{m_l,1}, a_{m_l,2}, \cdots, a_{m_l,N}\right)^T$ as the vectors of indication variables for power and subcarrier allocation, respectively. With the variables mentioned above, the RRM problem can be formulated as

$$\begin{aligned}
(\mathcal{P}_1)\ &\max_{\boldsymbol{P}_T,\boldsymbol{G},\boldsymbol{a}} \sum_{l=1}^{L}\sum_{m_l=1}^{M_l}\sum_{n=1}^{N} a_{m_l,n}C_{m_l,n} \\
&\text{subject to} \\
&\text{C1: } \left\|\boldsymbol{P}_{l,n,T}\right\|^2 = 1, \quad \forall l \in \mathcal{L}, n \in \mathcal{N} \\
&\text{C2: } \sum_{n=1}^{N} G_{l,n} \leq G_{l,max}, \quad \forall l \in \mathcal{L} \\
&\text{C3: } G_{l,n} \geq 0, \quad \forall l \in \mathcal{L}, n \in \mathcal{N} \\
&\text{C4: } \sum_{m_l=1}^{M_l} a_{m_l,n} \leq 1, \quad \forall l \in \mathcal{L}, n \in \mathcal{N} \\
&\text{C5: } a_{m_l,n} \in \{0,1\}, \quad \forall l \in \mathcal{L}, n \in \mathcal{N}
\end{aligned} \tag{7}$$

In the above formula, the objective function is to maximize system capacity of ultra-dense small cell networks by utilizing the maximum possible resources in polarization, power and frequency domains. C1 ensures that derived transmitting polarization states satisfy the modulus characteristics of Jones vector. Transmitting power is limited by transmit-power constraint given in C2, which is required to be positive by C3. C4 and C5 indicate that the subcarrier allocation in each small cell is constrained by OFDMA assumption.

There exist three kinds of decision variables in optimization problem $\mathcal{P}_1$, i.e., continuous variables including transmitting polarization states $\boldsymbol{P}_T$ and transmitting power $\boldsymbol{G}$, and discrete binary variable including subcarrier allocation variable $\boldsymbol{a}$. Therefore, $\mathcal{P}_1$ is a mixed integer non-convex problem, whose global optimum in closed form is difficult to derive. By dividing the RRM into three sub-problems, namely polarization state allocation, power allocation and subcarrier assignment, we propose a three-step iterative scheme named MC-JPPSA. It alternatively optimizes and assigns transmitting polarization states, power and subcarriers at every step. Though sub-optimal, the proposed scheme can obtain near-optimal performance with polynomial time complexity.

III. MULTICELL JOINT POLARIZATION, POWER AND SUBCARRIER ALLOCATION SCHEME

In this section, we will demonstrate the proposed MC-JPPSA scheme, which jointly utilizes polarization, power and frequency resources to fulfil the objective of system capacity maximization in ultra-dense small cell networks.

A. POLARIZATION STATE ALLOCATION

As distinguished from traditional RRM problem, spectrum opportunities in polarization domain are exploited in

MC-JPPSA scheme by means of optimizing transmitting polarization states of SBSs to maximize system capacity.

For given power vector $\boldsymbol{G}$ and subcarrier assignment vector $\boldsymbol{a}$, the polarization state allocation problem is transformed into

$$(\mathcal{P}_2)\ \max \sum_{l=1}^{L}\sum_{n=1}^{N}\log_2\left(1+\frac{G_{l,n}\left|(\boldsymbol{P}_{l,n,R})^H\boldsymbol{H}_{m_l^{[l,n]},l,n}\boldsymbol{P}_{l,n,T}\right|^2}{\sigma^2_{m_l^{[l,n]},n}+\sum_{i\neq l}^{L}G_{i,n}\left|(\boldsymbol{P}_{l,n,R})^H\boldsymbol{H}_{m_l^{[l,n]},i,n}\boldsymbol{P}_{i,n,T}\right|^2}\right)$$
$$s.t.\ \left\|\boldsymbol{P}_{l,n,T}\right\|^2=1,\quad \forall l\in\mathcal{L}, n\in\mathcal{N} \tag{8}$$

where $m_l^{[l,n]}=\arg\max_{m_l} a_{m_l,n}$.

Assume that $\frac{G_{l,n}\left|(\boldsymbol{P}_{l,n,R})^H\boldsymbol{H}_{m_l^{[l,n]},l,n}\boldsymbol{P}_{l,n,T}\right|^2}{\sigma^2_{m_l^{[l,n]},n}+\sum_{i\neq l}^{L}G_{i,n}\left|(\boldsymbol{P}_{l,n,R})^H\boldsymbol{H}_{m_l^{[l,n]},i,n}\boldsymbol{P}_{i,n,T}\right|^2}\gg 1$ holds which is benefited from the small coverage and thus high SINR of ultra-dense small cell networks. The objective function is approximated, and then $\mathcal{P}_2$ is simplified to

$$(\mathcal{P}_3)\quad \max \sum_{l=1}^{L}\sum_{n=1}^{N}\log_2\left(\frac{G_{l,n}(\boldsymbol{P}_{l,n,T})^H\boldsymbol{A}_{l,n}\boldsymbol{P}_{l,n,T}}{\sigma^2_{m_l^{[l,n]},n}+\sum_{i\neq l}^{L}G_{i,n}(\boldsymbol{P}_{i,n,T})^H\boldsymbol{B}_{l,n}\boldsymbol{P}_{i,n,T}}\right)$$
$$s.t.\ \left\|\boldsymbol{P}_{l,n,T}\right\|^2=1,\quad \forall l\in\mathcal{L}, n\in\mathcal{N} \tag{9}$$

where

$$\begin{cases}\boldsymbol{A}_{l,n}=(\boldsymbol{H}_{m_l^{[l,n]},l,n})^H\boldsymbol{P}_{l,n,R}(\boldsymbol{P}_{l,n,R})^H\boldsymbol{H}_{m_l^{[l,n]},l,n}\\ \boldsymbol{B}_{l,n}=(\boldsymbol{H}_{m_l^{[l,n]},i,n})^H\boldsymbol{P}_{l,n,R}(\boldsymbol{P}_{l,n,R})^H\boldsymbol{H}_{m_l^{[l,n]},i,n}\end{cases} \tag{10}$$

By relaxing the quadratical constraint of $\mathcal{P}_3$, a dual problem can be defined as follows

$$\min_{\boldsymbol{\lambda}} f(\boldsymbol{\lambda})\quad s.t.\ \boldsymbol{\lambda}\geq 0 \tag{11}$$

where $\boldsymbol{\lambda}=\{\lambda_{l,n}\}$, $\lambda_{l,n}$ denotes the Lagrange multiplier, and

$$f(\boldsymbol{\lambda})=\max_{\boldsymbol{P}_T} L(\boldsymbol{\lambda},\boldsymbol{P}_T) \tag{12}$$

The Lagrange function $L(\boldsymbol{\lambda},\boldsymbol{P}_T)$ is defined as

$$L(\boldsymbol{\lambda},\boldsymbol{P}_T)=\sum_{l=1}^{L}\sum_{n=1}^{N}\left\{\log_2\left(\frac{G_{l,n}(\boldsymbol{P}_{l,n,T})^H\boldsymbol{A}_{l,n}\boldsymbol{P}_{l,n,T}}{\sigma^2_{m_l^{[l,n]},n}+\sum_{i\neq l}^{L}G_{i,n}(\boldsymbol{P}_{i,n,T})^H\boldsymbol{B}_{l,n}\boldsymbol{P}_{i,n,T}}\right)-\lambda_{l,n}(\left\|\boldsymbol{P}_{l,n,T}\right\|^2-1)\right\} \tag{13}$$

The first-order derivative condition is derived by taking the derivative of $L(\boldsymbol{\lambda},\boldsymbol{P}_T)$ with respect to $\boldsymbol{P}_{l,n,T}$ as

$$\frac{\partial L(\boldsymbol{\lambda},\boldsymbol{P}_T)}{\partial \boldsymbol{P}_{l,n,T}}=\frac{2}{\ln 2}\frac{\boldsymbol{A}_{l,n}\boldsymbol{P}_{l,n,T}}{(\boldsymbol{P}_{l,n,T})^H\boldsymbol{A}_{l,n}\boldsymbol{P}_{l,n,T}}-2\lambda_{l,n}\boldsymbol{I}\boldsymbol{P}_{l,n,T}-\frac{2}{\ln 2}\sum_{i\neq l}^{L}\frac{G_{l,n}}{\sigma^2_{m_i^{[i,n]},n}+\sum_{j\neq i}^{L}G_{j,n}(\boldsymbol{P}_{j,n,T})^H\boldsymbol{B}_{j,n}\boldsymbol{P}_{j,n,T}}\boldsymbol{B}_{l,n}\times\boldsymbol{P}_{l,n,T} \tag{14}$$

where $\boldsymbol{I}$ represents identify matrix.

Assume that

$$\boldsymbol{K}_{l,n}=\sum_{i\neq l}^{L}\frac{G_{l,n}}{\sigma^2_{m_i^{[i,n]},n}+\sum_{j\neq i}^{L}G_{j,n}(\boldsymbol{P}_{j,n,T})^H\boldsymbol{B}_{j,n}\boldsymbol{P}_{j,n,T}}\boldsymbol{B}_{l,n}$$
$$\boldsymbol{T}_{l,n}=\boldsymbol{K}_{l,n}+\ln 2\lambda_{l,n}\boldsymbol{I} \tag{15}$$

The closed-form expressions for primal and dual variables $(\boldsymbol{P}_{l,n,T}{}^*,\lambda_{l,n}{}^*)$ are obtained as follows

$$\boldsymbol{P}_{l,n,T}{}^*=v_{\min}\left(\boldsymbol{A}_{l,n}{}^{-1}\boldsymbol{T}_{l,n}\right) \tag{16}$$
$$\lambda_{l,n}{}^*=\frac{1}{\ln 2}\left(1-(\boldsymbol{P}_{l,n,T})^H\boldsymbol{K}_{l,n}\boldsymbol{P}_{l,n,T}\right) \tag{17}$$

From (16), the transmitting polarization states of SBSs with subcarrier-based fashion are optimized, through which the spectrum opportunities in polarization domain are exploited for RRM in ultra-dense small cell networks. The polarization state allocation is conducted by executing Algorithm 1 which illustrates the detailed procedure of deriving transmitting polarization states in the kth iteration.

Algorithm 1 Polarization State Allocation

Input $\boldsymbol{a}[k-1]$, $\boldsymbol{G}[k-1]$, $\boldsymbol{P}_T[k-1]$.
Output $\boldsymbol{P}_T[k]$.
Repeat

- Calculate $\boldsymbol{A}_{l,n}$ and $\boldsymbol{B}_{l,n}$ according to (10).
- Substitute $\boldsymbol{B}_{l,n}$ into (15) to obtain $\boldsymbol{K}_{l,n}$ and $\boldsymbol{T}_{l,n}$.
- Update $\boldsymbol{P}_{l,n,T}[k]$ and $\lambda_{l,n}[k]$ based on (16) and (17), respectively.

Until $\|\boldsymbol{P}_T[k]-\boldsymbol{P}_T[k-1]\|<\varepsilon_P$ where $0<\varepsilon_P\ll 1$.

B. POLARIZATION-BASED POWER ALLOCATION

In this subsection, the polarization-based power allocation is proposed to further enhance system capacity. The distinction between traditional power allocation and the polarization-based power allocation is that the latter takes polarization into consideration so that polarization and power resources are jointly utilized.

Assuming that polarization state allocation and subcarrier assignment are fixed, transmitting power can be optimized through solving the following power allocation problem

$$(\mathcal{P}_4)\ \max \sum_{l=1}^{L}\sum_{n=1}^{N}\log_2 \times \left(1+\frac{G_{l,n}\left|(\boldsymbol{P}_{l,n,R})^H \boldsymbol{H}_{m_l[l,n],l,n}\boldsymbol{P}_{l,n,T}\right|^2}{\sigma^2_{m_l[l,n],n}+\sum_{i\neq l}^{L} G_{i,n}\left|(\boldsymbol{P}_{l,n,R})^H \boldsymbol{H}_{m_l[l,n],i,n}\boldsymbol{P}_{i,n,T}\right|^2}\right)$$
$$s.t.\ \sum_{n=1}^{N} G_{l,n}\leq G_{l,max},\quad \forall l\in\mathcal{L}$$
$$G_{l,n}\geq 0,\quad \forall l\in\mathcal{L}, n\in\mathcal{N} \tag{18}$$

Based on the Lagrange multiplier method, we can define the Lagrange function as follows

$$L(\boldsymbol{\beta},\boldsymbol{G}) = \sum_{l=1}^{L}\{\sum_{n=1}^{N}\log_2(\frac{G_{l,n}(\boldsymbol{P}_{l,n,T})^H \boldsymbol{A}_{l,n}\boldsymbol{P}_{l,n,T}}{\sigma^2_{m_l[l,n],n}+\sum_{i\neq l}^{L} G_{i,n}(\boldsymbol{P}_{i,n,T})^H \boldsymbol{B}_{l,n}\boldsymbol{P}_{i,n,T}}) + \beta_l(G_{l,max}-\sum_{n=1}^{N}G_{l,n})\} \tag{19}$$

where $\boldsymbol{\beta}=\{\beta_l\}$ is the vector of Lagrange multipliers.

Taking the first-order derivative of $L(\boldsymbol{\beta},\boldsymbol{G})$ with respect to $G_{l,n}$, we get

$$\frac{\partial L(\boldsymbol{\beta},\boldsymbol{G})}{\partial G_{l,n}} = \frac{1/\ln 2}{G_{l,n}+1/p_{l,n}} - \beta_l - r_{l,n} \tag{20}$$

where $p_{l,n}$ and $r_{l,n}$ denote the SINR and interference-related term of SBS l at subcarrier n, and are respectively defined as

$$p_{l,n} = \frac{\left|(\boldsymbol{P}_{l,n,R})^H \boldsymbol{H}_{m_l[l,n],l,n}\boldsymbol{P}_{l,n,T}\right|^2}{\sigma^2_{m_l[l,n],n}+\sum_{i\neq l}^{L} G_{i,n}\left|(\boldsymbol{P}_{l,n,R})^H \boldsymbol{H}_{m_l[l,n],i,n}\boldsymbol{P}_{i,n,T}\right|^2} \tag{21}$$

$$r_{l,n} = \sum_{i\neq l}^{L}\frac{G_{i,n}\left|(\boldsymbol{P}_{i,n,R})^H \boldsymbol{H}_{m_i[i,n],i,n}\boldsymbol{P}_{i,n,T}\right|^2}{\ln 2\,(1+G_{i,n}p_{i,n})} \times \frac{\left|(\boldsymbol{P}_{i,n,R})^H \boldsymbol{H}_{m_i[i,n],l,n}\boldsymbol{P}_{l,n,T}\right|^2}{(\sigma^2_{m_i[i,n],n}+\sum_{j\neq i}^{L} G_{j,n}\left|(\boldsymbol{P}_{i,n,R})^H \boldsymbol{H}_{m_j[j,n],j,n}\boldsymbol{P}_{j,n,T}\right|^2)^2} \tag{22}$$

The optimal transmitting power of SBS l at subcarrier n is given by

$$G^*_{l,n} = \left(\frac{1}{(\beta_l+r_{l,n})\ln 2} - 1/p_{l,n}\right)^+ \tag{23}$$

Note that the solution in (23) is a polarization-based water-filling power allocation policy which can be obtained by executing Algorithm 2. Compared with traditional power allocation schemes such as multicell improved iterative water filling (MC-IIWF) scheme in [23], the optimal power level of the polarization-based power allocation is related to not only the channel condition and noise power but also polarization states. The proposed polarization-based power allocation contributes to the utilization of polarization information and avoidance of performance degradation due to polarization mismatch [20].

Algorithm 2 Polarization-Based Water-Filling Power Allocation

Input $\boldsymbol{a}[k-1]$, $\boldsymbol{G}[k-1]$, $\boldsymbol{P}_T[k]$.
Output $\boldsymbol{G}[k]$.
Repeat
- Update $\{p_{l,n}\}$ and $\{r_{l,n}\}$ with (21) and (22), respectively.
- Obtain β_l via the bisection method.
- Calculate $\boldsymbol{G}[k]$ based on (23).

Until $\|\boldsymbol{G}[k]-\boldsymbol{G}[k-1]\| < \varepsilon_G$ where $0<\varepsilon_G\ll 1$.

C. SUBCARRIER ALLOCATION

In this subsection, we will demonstrate how to perform subcarrier allocation for given transmitting polarization state and power allocation. The subcarrier allocation problem can be formulated as

$$(\mathcal{P}_5)\ \max_{\boldsymbol{a}} \sum_{l=1}^{L}\sum_{m_l=1}^{M_l}\sum_{n=1}^{N} a_{m_l,n}C_{m_l,n}$$
$$s.t.\ \sum_{m_l=1}^{M_l} a_{m_l,n}\leq 1,\quad \forall l\in\mathcal{L}, n\in\mathcal{N}$$
$$a_{m_l,n}\in\{0,1\},\quad \forall l\in\mathcal{L}, n\in\mathcal{N} \tag{24}$$

The optimization problem (24) is an integer linear program, whose optimal solution is normally obtained by exhaustive search. Considering that the constraints are independent on different small cells, (24) can be decomposed into L subproblems. Without loss of generality, the subproblem of the lth SBS can be formulated as

$$(\mathcal{P}_6)\ \max_{a_{m_l,n}\in\{0,1\}} \sum_{m_l=1}^{M_l}\sum_{n=1}^{N} a_{m_l,n}C_{m_l,n}$$
$$s.t.\ \sum_{m_l=1}^{M_l} a_{m_l,n}\leq 1,\quad \forall n\in\mathcal{N} \tag{25}$$

By applying a greedy approach, each subcarrier is allocated to the SUE offering the maximum capacity at the subcarrier. That is, the optimal subcarrier assignment policy is obtained as

$$a_{m_l,n}{}^* = \begin{cases} 1, & \text{if } m_l = \arg\max C_{m_l,n} \\ 0, & \text{otherwise} \end{cases} \tag{26}$$

The proposed MC-JPPSA scheme maximizes the system capacity by jointly optimizing transmitting polarization state,

Algorithm 3 Iterative Polarization, Power and Subcarrier Allocation

Initialize $k \Leftarrow 0$, $\boldsymbol{G}[0]$, $\boldsymbol{P}_T[0]$.

Compute $\boldsymbol{a}[0]$ and $C[0]$ based on (26) and the objective function of (7), respectively.

Repeat 1)

1) Set $k \Leftarrow k+1$.
2) For fixed $\boldsymbol{a}[k-1]$ and $\boldsymbol{G}[k-1]$, calculate the optimal polarization state allocation $\boldsymbol{P}_T[k]$ with Algorithm 1.
3) For fixed $\boldsymbol{a}[k-1]$ and $\boldsymbol{P}_T[k]$, obtain the optimal power allocation $\boldsymbol{G}[k]$ by executing Algorithm 2.
4) Update subcarrier allocation $\boldsymbol{a}[k]$ by solving (26) with $\boldsymbol{P}_T[k]$ and $\boldsymbol{G}[k]$.
5) Compute $C[k]$ according to the objective function of (7).

Until $\frac{|C[k]-C[k-1]|}{C[k]} < \varepsilon$ where $0 < \varepsilon \ll 1$ or $k = K$.

power and subcarrier allocation with a three-step iterative approach. The detailed operations of MC-JPPSA scheme is described in Algorithm 3. After the iteration begins from $(\boldsymbol{P}_T[0], \boldsymbol{G}[0], \boldsymbol{a}[0])$, in the subsequent every iteration k, we find the optimal polarization state allocation vector $\boldsymbol{P}_T[k]$ for given $\boldsymbol{G}[k-1]$ and $\boldsymbol{a}[k-1]$ from the last iteration. Then we find the optimal power allocation vector $\boldsymbol{G}[k]$ with fixed $\boldsymbol{a}[k-1]$ and $\boldsymbol{P}_T[k]$. With $\boldsymbol{P}_T[k]$ and $\boldsymbol{G}[k]$, the optimal subcarrier allocation vector $\boldsymbol{a}[k]$ is updated. The iteration process ends until no further capacity improvement is achieved or the number of iterations exceeds the predefined K.

D. DISCUSSIONS

In this subsection, computational complexity, implementation issue and convergence property of the proposed scheme are discussed in detail.

1) COMPUTATIONAL COMPLEXITY

The computational complexity of MC-JPPSA scheme is discussed and compared with that of exhaustive search.

There exist three steps for the proposed scheme to solve the RRM problem: 1) polarization state allocation; 2) polarization-based power allocation; and 3) subcarrier allocation. Suppose that the number of iterations for finding ${\boldsymbol{P}_T}^*$ is T_1 in the polarization state allocation process; the complexity of the first step is $\mathcal{O}(T_1 LN)$. Given that the number of iterations needed in polarization-based power allocation is T_2, the second step based on water-filling policy has a known complexity of $\mathcal{O}\left[T_2 LN \log_2(N)\right]$ [24]. By applying a greedy approach, subcarrier assignment has a complexity of $\mathcal{O}\left(N \sum_{l=1}^{L} M_l\right)$. Let T_3 be the number of iterations required for scheme stopping; thus, the total complexity of MC-JPPSA scheme is $O\left\{T_3\left[T_1 LN + T_2 LN \log_2(N) + N\sum_{l=1}^{L} M_l\right]\right\}$. Since T_1, T_2 and T_3 are polynomial functions of N which is usually large in realistic wireless communication systems, the proposed MC-JPPSA scheme can be executed in polynomial time.

On the other hand, the optimal exhaustive search is implemented by optimal power and subcarrier allocation searching, and two-dimensional optimal transmitting polarization state searching including amplitude ratio and relative phase searching. The complexity of exhaustive search is in exponential time $\mathcal{O}\left[\left(N_G N_{\gamma_T} N_{\phi_T}\right)^{LN}\left(\prod_{l=1}^{L} M_l\right)^N\right]$, where N_G, N_{γ_T} and N_{ϕ_T} are the numbers of transmitting power, amplitude ratio and relative phase descriptors searched at every subcarrier of every SBS, respectively. With the increase of searching precision and N, the complexity of exhaustive search improves sharply and is much higher than that of the proposed scheme.

2) IMPLEMENTATION

The proposed MC-JPPSA scheme is implemented in a centralized manner by employing a central node which is more powerful for system capacity optimization than the easy-implemented distributed manner.

The main concern in implementation is generating transmitting polarization states with subcarrier-based fashion. Since ODPAs determine polarization states physically based on antenna configuration, it is not practical to arbitrarily generate transmitting polarization states by ODPAs owing to the complex hardware structure. To generate the optimal transmitting polarization states of SBSs at every subcarrier, virtual polarization adaptation (VPA) method [21] is adopted which employs digital signal processing in the processor to generate polarization states digitally.

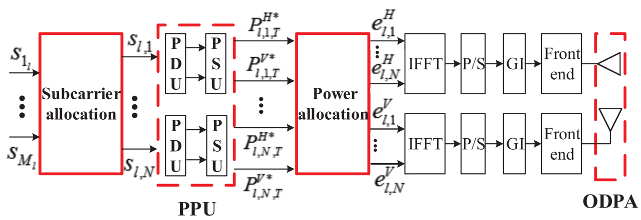

FIGURE 3. Transmitter structure for MC-JPPSA scheme.

Fig. 3 shows the transmitter structure of the lth SBS for MC-JPPSA scheme. Assume that after subcarrier allocation, the signal $s_{l,n}$ at subcarrier n is transmitted with polarization state ${\boldsymbol{P}_{l,n,T}}^* = \left({P^H_{l,n,T}}^*, {P^V_{l,n,T}}^*\right)^T$. Based on VPA method, ${\boldsymbol{P}_{l,n,T}}^*$ is generated by a digital signal processing branch at SBS, that is, a power processing unit (PPU) comprised of power division unit (PDU) and phase shift unit (PSU). The following power allocation module executes the polarization-based power allocation. ODPAs equipped on SBS are responsible for transmitting polarized signals to the SUEs.

3) CONVERGENCE

Convergence is an important property of iterative schemes. For the proposed MC-JPPSA scheme, subcarrier allocation is accomplished by solving integer linear program directly without iterations and thus can be ignored in convergence analysis. As illustrated in [23], the convergence property of traditional modified iterative water-filling scheme is difficult to prove theoretically in full generality. Furthermore, since the transmitting polarization states are recalculated by Algorithm 1 in every iteration, the polarization-based power allocation is time-varying over iterations. Therefore, it is very challenging to prove the convergence property of the proposed scheme under a time-varying mapping function [25]. Nevertheless, convergence of the proposed scheme has always been observed in our simulations.

IV. NUMERICAL SIMULATIONS

In this section, simulation results are provided to evaluate the performance of MC-JPPSA scheme. We take three schemes as reference: the optimal exhaustive search, multi-cell improved iterative water filling (MC-IIWF) scheme [23] as an example of traditional joint power and subcarrier allocation schemes, and joint polarization and power allocation (JPPA) scheme [20] implemented at each SBS separately so as to ensure comparability.

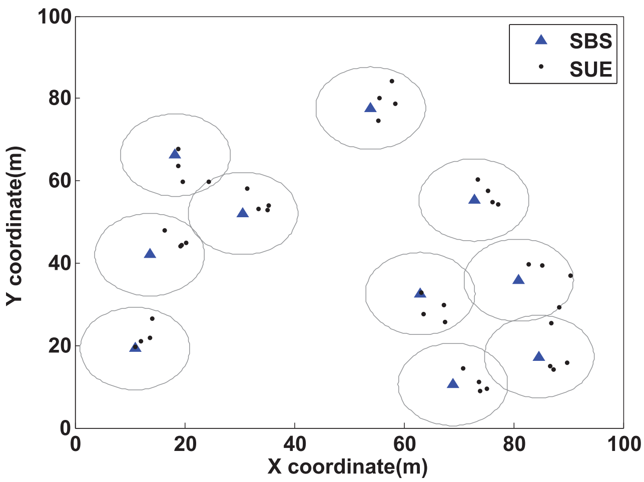

FIGURE 4. Network topology in the simulation.

A. SIMULATION CONFIGURATION

We consider a ultra-dense network topology in the simulation as shown in Fig. 4. As a typical case of dense environments, the SBSs are randomly distributed in a rectangular region with the size of 100 m × 100 m. In each small cell, the SBS is allocated in the center of a circle area with the diameter of 20 m. In addition, all the SUEs randomly distributed in their own small cells.

SBSs and SUEs are equipped with ODPAs, and the multi-path parameters of dual-polarized frequency-selective fading channels are set according to IMT-Advanced channel model in ITU-R M.2135 [26]. Main simulation parameters are provided in Table I based on 3GPP evaluation methodology [27].

B. SIMULATION RESULTS

In this subsection, the performance of MC-JPPSA scheme is evaluated through computational complexity and convergence analysis, and then comparisons with existing MC-IIWF and JPPA schemes.

TABLE 1. Simulation parameters.

Parameter	Value
Carrier frequency	2 GHz
System bandwidth	10 MHz
Transmit-power constraint	$20dBm \sim 40dBm$
Number of small cells	$2 \sim 10$
Number of SUEs	$2 \sim 10$
Data modulation	OFDM $\pi/4 - QPSK$
Useful symbol time	$6.4 \times 10^{-6}s$
Guard interval	$1.25 \times 10^{-6}s$

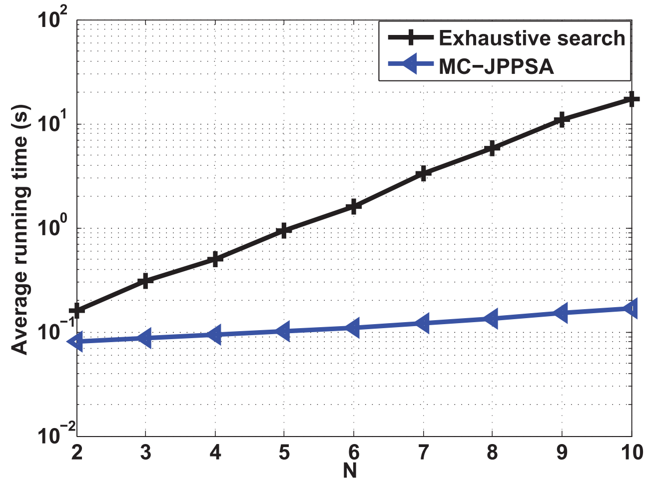

(a)

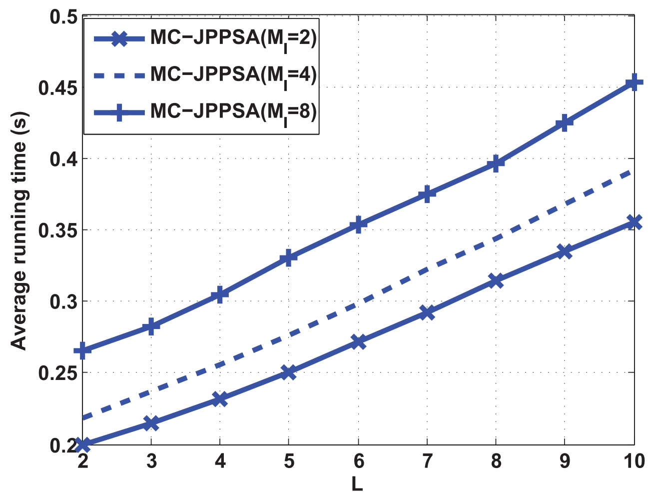

(b)

FIGURE 5. Average running time evaluation versus (a) the number of subcarriers, (b) the number of small cells.

1) ANALYSIS OF THE PROPOSED SCHEME

a: COMPUTATIONAL COMPLEXITY

In Fig. 5(a) and 5(b), the average running time of MC-JPPSA scheme versus the numbers of subcarriers and small cells are depicted, respectively. Assume that the number of SUEs in every small cell is equal without loss of generality. The simulations are run on a personal computer with hardware and software conditions: Windows 7 Professional Edition, Pentium(R) 2.9 GHz Processor, 4 GB RAM.

Fig. 5(a) evaluates the average running time of MC-JPPSA scheme through comparison with the optimal exhaustive search. Since exhaustive search suffers high computation cost, we fix $L = M_l = 4$ and choose a small number of subcarriers to run the simulation. With the increasing number of subcarriers, the average running time of exhaustive search grows exponentially, which is obviously higher than that of MC-JPPSA scheme. Fig. 5(b) shows the average running time of MC-JPPSA scheme with $N = 32$ under different numbers of small cells. The average running time of MC-JPPSA scheme increases with L and M_l. Even under $L = 10, M_l = 8$ and $N = 32$, MC-JPPSA takes about 0.45 s for resource allocation. It is much more efficient than exhaustive search under $L = 10, M_l = 4$ and $N = 4$ which takes 18 s according to Fig. 5(a).

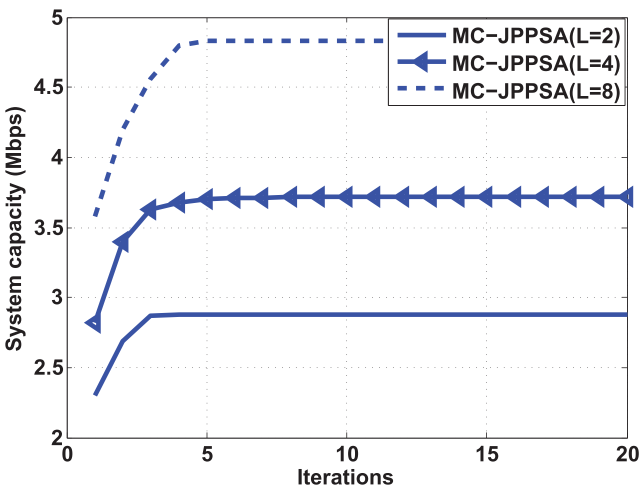

FIGURE 6. System capacity versus the number of iterations for MC-JPPSA scheme.

b: CONVERGENCE

In Fig. 6, we present the convergence process of MC-JPPSA scheme by plotting the system capacity versus the number of iterations when $M_l = 4$ and $N = 64$. For any reported value of L, only 4∼6 iterations are needed to achieve most of the system capacity. Though increased L slows down the convergence speed slightly, the proposed scheme still presents short convergence time. Therefore, MC-JPPSA scheme can optimize system capacity in a timely fashion, which makes the proposed scheme suitable for highly delay-sensitive wireless communication environment.

2) COMPARISONS WITH KNOWN SCHEMES

a: TRANSMIT-POWER CONSTRAINT

Fig. 7 evaluates the system capacity against transmit-power constraint $G_{l,max}$ with $L = 4$, $M_l = 4$ and $N = 64$. For simplicity, $G_{l,max}$ is assumed to be identical for all

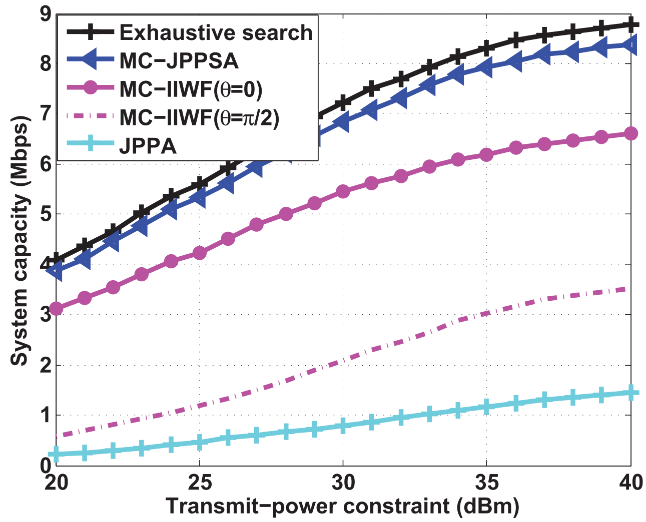

FIGURE 7. System capacity versus transmit-power constraint.

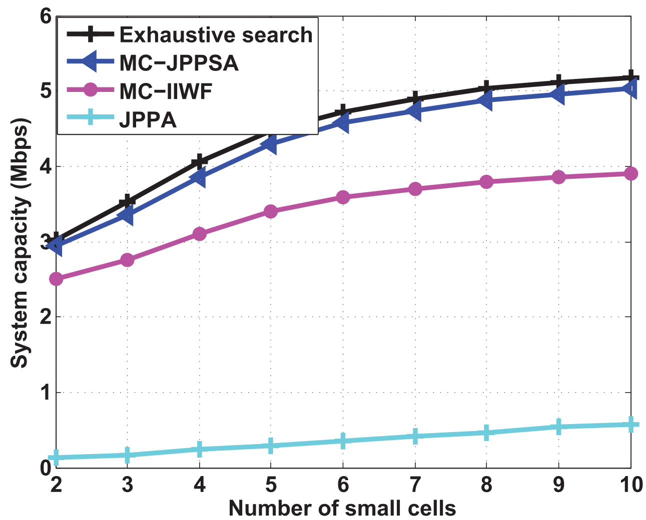

FIGURE 8. System capacity versus the number of small cells.

the small cells. It is obvious that with the increase of $G_{l,max}$, higher system capacity can be achieved by utilizing more power resources. The performance of exhaustive search serves as the upper bound at the expense of high computational complexity as illustrated in Fig. 5(a). Benefited from the utilization of polarization resources in ultra-dense small cell networks, the proposed MC-JPPSA scheme outperforms traditional MC-IIWF scheme, and approaches exhaustive search with much lower complexity. The system capacity of MC-IIWF scheme decreases due to the impairment from polarization mismatch. Polarization mismatch is caused by channel depolarization effect and different antenna configurations between transmitting and receiving antennas, and measured by polarization mismatch angle θ. Compared with ideal case ($\theta = 0$), worst case ($\theta = \pi/2$) with severe polarization mismatch yields large performance degradation of MC-IIWF scheme, which

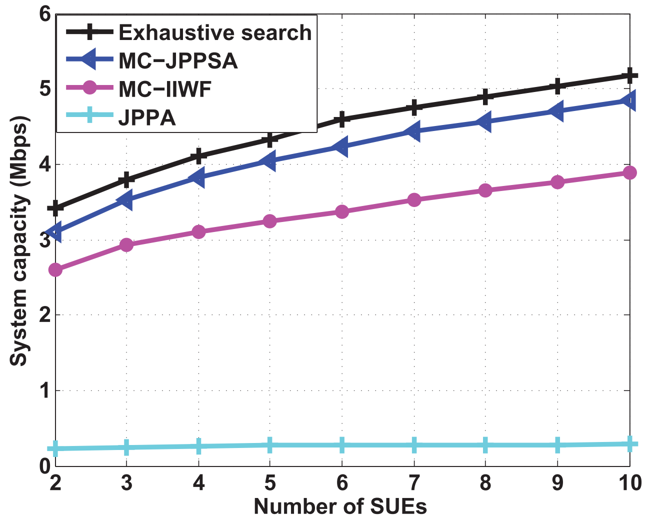

(a)

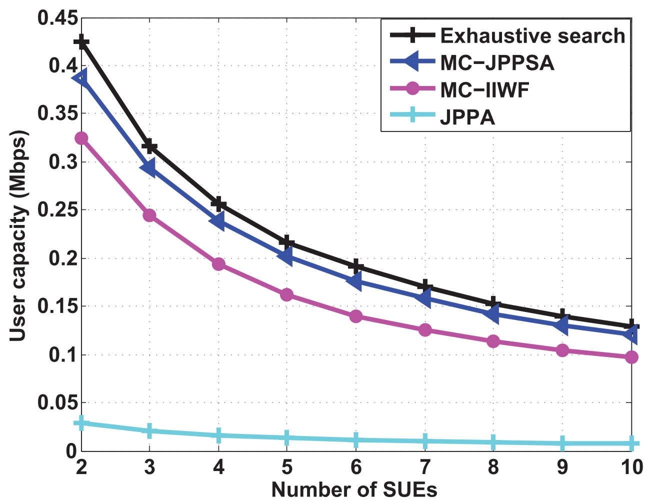

(b)

FIGURE 9. Influence of the number of SUEs on (a) system capacity and (b) user capacity.

indicates the necessity of taking polarization into consideration. JPPA scheme provides the lower bound of system capacity, since it is implemented in each small cell separately without coordination and thus suffers from severe inter-cell interference.

b: NUMBER OF SMALL CELLS

System capacity with respect to the number of small cells is evaluated in Fig. 8 under $M_l = 4$ and $N = 64$. Exhaustive search and JPPA provide the upper and lower bound of system capacity performance, respectively. By optimizing transmitting polarization states, the proposed MC-JPPSA scheme achieves higher performance than MC-IIWF. As shown in Fig. 8, the system capacities of all schemes increase when small cell networks become denser by increasing the number of small cells L. This is because that increasing the number of small cells within a certain region can shorten the distance between SUEs and SBSs, increase the power of received target signal for SUEs, and improve the SINR of downlink communication. As the number of small cells increases further, the increase of achieved system capacity tends to be gentle and gradually reaches saturation.

c: NUMBER OF SUEs

The influence of the number of SUEs M_l on system capacity and user capacity is illustrated in Fig. 9(a) and 9(b) under $L = 4$ and $N = 64$, respectively. Fig. 9(a) shows that when M_l increases from 2 to 10, the system capacities are improved for all the schemes due to multiuser diversity effect. In a fading environment, increasing the number of SUEs can increase the chance of accessing the channels with higher channel quality for SUEs and thus achieves higher system capacity. Also, the proposed MC-JPPSA scheme can improve the system capacity over MC-IIWF scheme by 15% $\sim$ 20%, which verifies the benefit of exploiting polarization for resource allocation in ultra-dense small cell networks. From Fig. 9(b), we can observe that the downlink capacity of each user named user capacity decreases with the increasing number of SUEs. That is, the performance of a single SUE degrades as the number of SUEs increases, which implies that the system capacity gain benefited from multiuser diversity effect does not increase linearly with the number of SUEs in ultra-dense deployment scenario.

V. CONCLUSIONS

In this paper, we exploit polarization as a novel means for system capacity enhancement in ultra-dense small cell networks, and propose a multicell joint polarization, power and subcarrier allocation scheme by joint utilization of polarization, power and frequency resources. The radio resource management problem is formulated as a mixed integer non-convex optimization problem. And sub-optimal solutions are derived by employing an iterative approach where transmitting polarization states, power and subcarriers are optimized iteratively. Simulation results verify that the proposed scheme can offer system capacity performance close to the optimal exhaustive search with much lower computational complexity, and outperforms the traditional joint power and subcarrier allocation scheme. We have shown that leveraging polarization has a great application prospect to realize high system capacity in ultra-dense small cell networks which is the main trend of future wireless communication systems.

In the next step, polarization resource utilization based on a distributed manner will be studied in ultra-dense small cell networks. Though the proposed scheme based on a centralized manner achieves great performance gains, a distributed scheme may be more preferred in some practical cases where employing a central node is impractical.

REFERENCES

[1] Cisco. "Cisco visual networking index: Global mobile data traffic forecast update, 2015-2020," Cisco, San Jose, CA, USA, White Paper, 2016. [Online]. Available: http://www.cisco.com/c/en/us/solutions/collateral/service-provider/visual-networking-index-vni/mobile-white-paper-c11-520862.html

[2] Ericsson, "5G radio access-research and vision," Ericsson, Stockholm, Sweden, White Paper, 2013.
[3] M. Kamel, W. Hamouda, and A. Youssef, "Ultra-dense networks: A survey," *IEEE Commun. Mag.*, vol. 18, no. 4, pp. 2522–2545, Apr. 2016.
[4] D. T. Ngo, S. Khakurel, and T. Le-Ngoc, "Joint subchannel assignment and power allocation for OFDMA femtocell networks," *IEEE Trans. Wireless Commun.*, vol. 13, no. 1, pp. 342–355, Jan. 2014.
[5] M. Ozawa and T. Ohtsuki, "Improvements of femto-base station resource utilisation and ABS assignment convergence for dynamic ABS assignment," *IET Commun.*, vol. 11, no. 3, pp. 370–376, Mar. 2017.
[6] A. R. Elsherif, W. P. Chen, A. Ito, and Z. Ding, "Adaptive resource allocation for interference management in small cell networks," *IEEE Trans. Commun.*, vol. 63, no. 6, pp. 2107–2125, Jun. 2015.
[7] E. G. Larsson, O. Edfors, F. Tufvesson, and T. L. Marzetta, "Massive MIMO for next generation wireless systems," *IEEE Commun. Mag.*, vol. 52, no. 2, pp. 186–195, Feb. 2014.
[8] Z. Luan, H. Qu, J. Zhao, B. Chen, and J. C. Principe, "Correntropy induced joint power and admission control algorithm for dense small cell network," *IET Commun.*, vol. 10, no. 16, pp. 2154–2161, Mar. 2016.
[9] C. Guo, F. Liu, S. Chen, C. Feng, and Z. Zeng, "Advances on exploiting polarization in wireless communications: Channels, technologies, and applications," *IEEE Commun. Surveys Tuts.*, vol. 19, no. 1, pp. 125–166, 1st Quart, 2016.
[10] X.-W. Dai, Z.-Y. Wang, C.-H. Liang, X. Chen, and L.-T. Wang, "Multiband and dual-polarized omnidirectional antenna for 2G/3G/LTE application," *IEEE Antennas Wireless Propag. Lett.*, vol. 12, pp. 1492–1495, 2013.
[11] D. Li, C. Guo, Z. Zeng, and X. Lin, "A novel underlay TV spectrum sharing scheme based on polarization adaption for TD-LTE system," in *Proc. Wireless Commun. Netw. Conf*, 2013, pp. 2484–2489.
[12] D. Li, Z. Zeng, C. Guo, and X. Lin, "Cluster-based polarized spectrum sharing in channels with polarization mode dispersion," *ETRI J.*, vol. 36, no. 3, pp. 502–505, 2014.
[13] D. Li, Z. Sun, Z. Zeng, C. Guo, and X. Lin, "A novel semi-blind polarization adaption technique for cognitive users," *IEEE Commun. Lett.*, vol. 19, no. 4, pp. 681–684, Apr. 2015.
[14] X. Lin, C. Guo, Z. Zeng, and D. Li, "A novel interference avoidance scheme based on blind polarization signal processing for cognitive Femtocell network," in *Proc. Int. Symp. Wireless Pers. Multimedia Commun.*, 2012, pp. 40–44.
[15] J.-M. Dricot, P. De Doncker, and F. Horlin, "On the co-existence of dual-polarized CDMA networks," in *Proc. 4th Int. Conf. Cognit. Radio Oriented Wireless Netw. Commun.*, 2009, pp. 1–6.
[16] B. Cao, H. Liang, J. W. Mark, and Q. Zhang, "Exploiting orthogonally dual-polarized antennas in cooperative cognitive radio networking," *IEEE J. Sel. Areas Commun.*, vol. 31, no. 11, pp. 2362–2373, Nov. 2013.
[17] Q. Zhang, B. Cao, Y. Wang, and N. Zhang, "On exploiting polarization for energy-harvesting enabled cooperative cognitive radio networking," *IEEE Wireless Commun.*, vol. 20, no. 4, pp. 116–124, Apr. 2013.
[18] B. Cao, Q. Zhang, R. Lu, and J. W. Mark, "PEACE: Polarization enabled active cooperation scheme between primary and secondary networks," *IEEE Trans. Veh. Technol.*, vol. 63, no. 8, pp. 3677–3688, Oct. 2014.
[19] S. Chen, Z. Zeng, and C. Guo, "Exploiting polarization for underlay spectrum sharing in cognitive heterogeneous cellular network," in *Proc. IEEE GLOBECOM*, 2016, pp. 1–6.
[20] S. Chen, Z. Zeng, and C. Guo, "Polarization and power optimization for spectrum sharing in cognitive heterogeneous cellular network," in *Proc. IEEE WCNC*, Dec. 2017, pp. 1–6.
[21] A. J. Poelman, "Virtual polarization adaptation a method of increasing the detection capability of a radar system through polarization-vector processing," *IEEE Proc.-F. Commun., Radar Signal Process.*, vol. 128, no. 5, pp. 261–270, May 1981.
[22] T. Pratt, B. Walkenhorst, and S. Nguyen, "Adaptive polarization transmission of OFDM signals in a channel with polarization mode dispersion and polarization dependent loss," *IEEE Trans. Wireless Commun.*, vol. 8, no. 7, pp. 3354–3359, Jul. 2009.
[23] L. Venturino, N. Prasad, and X. Wang, "Coordinated scheduling and power allocation in downlink multicell OFDMA networks," *IEEE Trans. Veh. Technol.*, vol. 58, no. 6, pp. 2835–2848, Jul. 2009.
[24] W. Yu and R. Lui, "Dual methods for nonconvex spectrum optimization of multicarrier systems," *IEEE Trans. Commun.*, vol. 54, no. 7, pp. 1310–1322, Jul. 2006.
[25] Z. Yin, F. R. Yu, S. Bu, and Z. Han, "Joint cloud and wireless networks operations in mobile cloud computing environments with telecom operator cloud," *IEEE Trans. Wireless Commun.*, vol. 14, no. 7, pp. 4020–4033, Jul. 2015.
[26] "Guidelines for evaluation of radio interface technologies for IMT-advanced," ITU-R, Geneva, Switzerland, Tech. Rep. ITU-R M.2135, 2008.
[27] *Evolved Universal Terrestrial Radio Access (E-UTRA): Further advancements for E-UTRA physical layer aspects*, Document TR 36.814, Third-Generation Partnership Project, 2010.

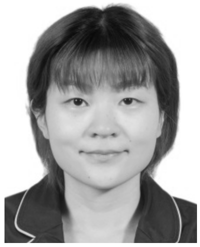

SHUO CHEN received the B.S. degree in telecommunication engineering and management from the Beijing University of Posts and Telecommunications (BUPT), Beijing, China, and the master's degree in electronics engineering from the Queen Mary University of London, London, U.K., in 2012. She is currently pursuing the Ph.D. degree in information and communication engineering with BUPT. Her current research interests are in the areas of wireless communications and networks, with an emphasis on cognitive radios and spectrum sharing.

ZHIMIN ZENG received the B.S. degree in carrier communication, the M.S. degree in communication and electronic systems, and the Ph.D. degree in communication and information systems from the Beijing University of Posts and Telecommunications (BUPT), Beijing, China. He is currently a Professor with the School of Information and Communication Engineering, BUPT. He is a Senior Member of the China Institute of Communications, an Advanced Member of the Chinese Institute of Electronics, and a member of the Academic Committee of BUPT. His current research interests include theory and technology of next-generation mobile and wireless networks.

CAILI GUO received the Ph.D. degree in communication and information systems from the Beijing University of Posts and Telecommunications (BUPT), Beijing, China, in 2008. She is currently a Professor with the School of Information and Communication Engineering, BUPT. Her research interests are in the areas of wireless communications and networks, with an emphasis on spectrum sharing and cognitive radios.